Available online at www.sciencedirect.com
ScienceDirect
Carbohydrate Polymers 73 (2008) 156–163
Carbohydrate Polymers
www.elsevier.com/locate/carbpol

Changes in fiber ultrastructure during various kraft pulping conditions evaluated by ^{13}C CPMAS NMR spectroscopy

Tommi Virtanen [a,*], Sirkka Liisa Maunu [a], Tarja Tamminen [b], Bo Hortling [c], Tiina Liitiä [c]

[a] *Laboratory of Polymer Chemistry, P.O. Box 55, FIN-00014, University of Helsinki, Finland*
[b] *VTT, P.O. Box 1000, FIN-02044 VTT, Finland*
[c] *KCL, P.O. Box 70, FI-02151 Espoo, Finland*

Received 5 February 2007; received in revised form 5 October 2007; accepted 14 November 2007
Available online 22 November 2007

Abstract

In order to obtain information about the correlation of cellulose fibril aggregate size with the macroscale properties of the wood pulp fibers, three kraft cooking methods with widely varying cooking conditions were used to produce kraft pulps having significantly different physical properties. Variations in cooking conditions included different cooking temperatures, and changes in alkalinity and sulfidity levels. The ultrastructure of these kraft pulps was analysed using ^{13}C CPMAS NMR spectroscopy. From measured spectra cellulose fibril aggregate sizes were determined by means of deconvolution. It was observed that changes in kraft pulping conditions have effect on aggregate size in studied pulps. No clear correlation however between aggregate sizes and physical properties of the pulps was observed.

Keywords: ^{13}C CPMAS NMR; Cellulose; Fibril aggregation; Kraft pulp; Deconvolution

1 Introduction

In wood cell wall cellulose chains are grouped together to form cellulose fibrils, which in turn form larger structures known as fibril aggregates (Fig. 1). The shape and average size of these aggregates have been earlier studied by using different spectroscopic and microscopic methods (Duchesne & Daniel, 2000; Fahlen & Salmen, 2003; Hult, Iversen, & Sugiyama, 2003; Newman, 1999a), and computer models for fibril morphology have also been presented (Baird, O'Sullivan, & Banks, 1998). Fibril aggregation influences reactivity of cellulose substrates in chemical modification of cellulose, also the susceptibility of cellulose substrates to enzymatic hydrolysis is affected (Krässig, 1993; Samejima, Sugiyama, Igarashi, & Eriksson, 1998). However it is not very well understood how fibril aggregation affects the macroscale properties of pulp, for example to the strength properties of the fiber. It is therefore not clear if large fibril aggregate size is really a desirable property for a fiber to have.

The ultrastructure of cellulose from various sources (wood, bacterial cellulose, and pulps produced with different pulping methods) has been studied extensively lately. Methods that have been applied include transmission electron microscopy (TEM) (Bardage, Donaldson, Tokoh, & Daniel, 2004; Duchesne, Takabe, & Daniel, 2003), field emission scanning electron microscopy (FE-SEM) (Duchesne & Daniel, 2000), atomic force microscopy (AFM) (Fahlen & Salmen, 2003; Fahlen & Salmen, 2005), wide-angle X-ray scattering (WAXS) (Newman, 1999a) and solid state ^{13}C cross polarization magic angle spinning (CPMAS) NMR spectroscopy (Atalla & VanderHart, 1999; Hult, Liitiä, Maunu, Hortling, & Iversen, 2002; Hult et al., 2003). Reported values for cellulose fibril aggregates in kraft pulps vary from 15 to 25 nanometers. The advantage of different microscopic methods when used to characterize the cellulose fibril aggregate sizes is the full size distribution of aggregates that is obtained. However non-cellulosic polysaccharides that are present at the fibril sur-

* Corresponding author. Tel.: +358 9 1915 0339; fax: +358 9 1915 0330.
E-mail address: tommi.virtanen@helsinki.fi (T. Virtanen).

0144-8617/$ - see front matter © 2007 Elsevier Ltd. All rights reserved.
doi:10.1016/j.carbpol.2007.11.015

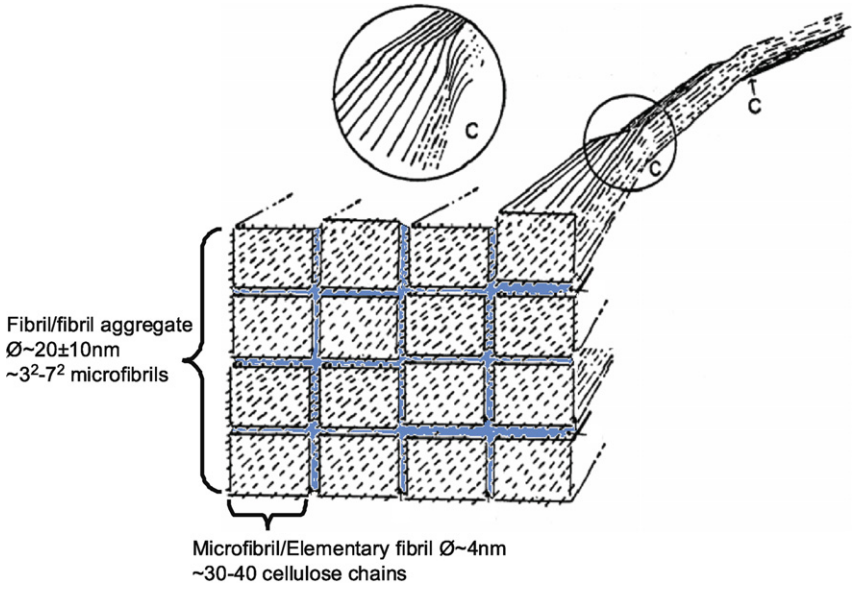

Fig. 1. Cellulose fibril aggregate (adapted from the Ph.D. thesis of Wathen (2006)).

faces may affect the result. When replication techniques are used in combination with electron microscopy, the sample preparement also requires some effort.

Solid state ^{13}C CPMAS NMR spectroscopy is a versatile tool for morphology studies of cellulosic materials. The resolution of ^{13}C CPMAS NMR spectra is adequate enough to allow chemically equivalent carbons from different magnetic environments to be separated, however special techniques like deconvolution are needed to fully interpret the strongly overlapping lines. Highly informative region in ^{13}C spectrum is the signal from C(4) carbon at ~80–90 ppm. From this resonance one can easily distinguish separate signals originating from crystalline and non-crystalline cellulose. Information extracted from this region can be used to determine for example the crystallinity of cellulose (Liitiä, Maunu, & Hortling, 2000; Newman & Hemmingson, 1990; Teeäär, Serimaa, & Paakkari, 1987), relative amounts of different cellulose allomorphs present (Lennholm, Larsson, & Iversen, 1994; Newman, 1999b; Yamamoto & Horii, 1993), or to calculate lateral dimensions for cellulose fibrils and fibril aggregates. Values obtained earlier for lateral dimensions of cellulose fibrils and fibril aggregates with ^{13}C CPMAS NMR are in good accordance with those obtained with different microscopic and X-ray scattering methods (Duchesne et al., 2001; Hult et al., 2003; Newman, 1999a). These values for lateral dimensions obtained with ^{13}C CPMAS NMR are however averages over the whole cell wall, and it is therefore not possible to obtain specified information from different cell wall layers.

During chemical pulping wood cell wall components are partially dissolved and changes in ultrastructure of fibers take place. Crystallinity of cellulose increases, and there is also an increase in lateral fibril aggregate dimension (Duchesne & Daniel, 2000; Evans, Newman, Roick, Suckling, & Wallis, 1995; Fahlen & Salmen, 2003; Hult et al., 2003). It is believed that this enlargement of fibril aggregates is mainly due to additional freedom of organization gained by removal of hemicelluloses (Duchesne et al., 2001; Hult, Larsson, & Iversen, 2001), but there is also evidence that elevated temperature in pulping process is a more crucial factor for aggregate growth than the amount of hemicelluloses in fiber (Fahlen & Salmen, 2003; Fahlen & Salmen, 2005).

Variations in pine kraft pulp properties are mainly affected by cooking conditions when the wood raw material is constant. There are certain known effects of cooking conditions on cooking selectivity and further on pulp properties. However, unambiguous knowledge about the connections between the chemical and physical changes in fibers and the changes in pulp properties is still lacking. The composition of the pulp components can be analysed by standard procedures, but the interactions between the components (e.g. cellulose fibril aggregation) are more difficult to analyse. However, these interactions are expected to affect pulp properties and are thus of interest.

In the present study, various alkaline pulping methods were applied. High temperature and high alkalinity enabled the cooking to proceed very fast, whereas low sulfidity was used to produce a pulp requiring long cooking time. Profiled alkalinity in cooking was used to reach a pulp of high quality. As reference, standard cooking conditions were applied. The comparison between the pulps was performed at two kappa number levels. In high alkalinity cooks, the effects of cooking temperature, impregnation conditions and the addition of polysulfide were studied by varying these parameters, while keeping other cooking parameters constant. Both the effects on pulp properties and cellulose fibril aggregate size were analysed, aiming at finding correlations between them. Furthermore the effect of bleaching

on aggregate structure was evaluated within this study by analysing samples from different cooking experiments bleached with ODEDED-sequence. Aggregation analysis was done using ^{13}C solid state CPMAS NMR spectroscopy combined with deconvolution of spectral data. Both the fitting method and cellulose isolation technique were similar to those used by Hult et al. (2002).

2. Materials

2.1. Cooking

Pine (Pinus sylvestris) from southeastern Finland was used. Cooks to kappa level 30 were performed in large scale in a 30 L digester using mill chips. The chip charge was 4500 g (o.d.) and the liquor-to-wood ratio 4 during the impregnation step and 5 during the cooking stage. In addition, some cooks were performed to kappa level 50 in small scale in rotating 1 L autoclaves in an air bath. In this case, chip dimensions were 2–3 mm × 20 mm × 30 mm. Chip charge was 100 g (o.d.) and liquor-to-wood ratio 4 during the impregnation step and 5 during the cooking stage. The impregnation and cooking conditions of the pulps are given in Table 1, and the properties of the pulps in Tables 2 and 7. ISO-standards concerning the methods used for measuring the physical properties are given in Table 3. The reference cooks (Ref) were performed by a good normal practice of kraft cooking. The high alkalinity cooks (HiA) were rapid cooks due to the high alkali charge and high temperature, while the low sulfidity cook (LS) was the slowest cooking method.

2.2. ODEDED bleaching

Oxygen delignification was performed to the pulps at kappa level 30 in modified Quantum Mark II fluidising reactor. Pulp charge was 320 g (o.d.), consistency 12%, temperature 90 °C, time at 90 °C 60 min and oxygen pressure 8 bar. The $MgSO_4$ concentration was 0.5% and the NaOH concentration 0.065–0.070* (unbleached kappa number of pulp). The oxygen delignified pine kraft pulps were bleached to target brightness of 89% by DEDED sequence using conventional laboratory technique.

Table 2
Properties of the pulps

	Kappa number	Brightness (%)	Viscosity (ml/mg)	Yield (%)
LS	29.8	28.1	1020	44.5
Ref[a]	31.9/50.6	30.6/23.9	1350/1440	46.5/50.0
HiA130i180c[a]	33.7/45.2	35.5/33.6	1070/NA	43.9/45.4
HiA90i180c	31.9	36.8	960	43.5
HiA90i160c	32.3	35.7	1170	43.9
PS	32.3	26.5	1340	47.0
PS-HiA	33.2	35.2	1120	47.7

[a] Higher/lower H factor, see Table 1.

Table 3
ISO standards for methods used in analysis of pulp properties

Brightness	ISO 2470
Viscosity	ISO 5351/1
Kappa number	ISO 302
Water retention value (WRV)	ISO 5267-2
Density	ISO 534
Tear index	EN ISO 5270
Zero-span tensile index, wet	ISO 15361
Scott bond	TAPPI T 833 motif

3. Experimental

3.1. NMR methods

Solid state CPMAS ^{13}C NMR spectra were measured for high alkalinity, low sulfidity and reference pulp samples. From high alkalinity and reference pulps samples from kappa levels 30 and 50 were included. From high alkalinity cook a series of samples differing in cooking temperature and impregnation conditions, and also with added polysulfide (PS) were analysed. All spectra were measured from never-dried samples with water content determined after measurement to be over 40% by weight.

For successful spectral fitting it is important to remove non-cellulosic materials that contribute to the C(4)-spectral region of cellulose. All samples were therefore subjected to strong acid hydrolysis in order to remove hemicelluloses. Prior acid hydrolysis the residual lignin in unbleached samples was also removed using chlorite treatment. These pre-

Table 1
Impregnation and cooking conditions

	Impregnation (i)				Cooking (c)			
	Temp (°C)	Time (min)	Eff. Alkali (mol/kg)	Sulfidity (%)	Temp (°C)	Eff. Alkali (mol/kg)	Sulfidity (%)	H factor
LS	130	60	3.5	10.8	160	1.5	0	5000
Ref	130	60	3.5	40	160	1.5	40	1000[a]/1507
HiA130i180c	130	60	4	40	180	6	40	350[a]/600
HiA90i180c	90	120	4	40	180	6	40	478
HiA90i160c	90	120	4	40	160	6	40	507
PS	130	60	3.5	20	160	1.5	20	2206
PS-HiA	90	120	4	20	180	6	20	399

[a] Target kappa number 50, in other cases 30.

treatments of the samples were performed following the methods introduced by Hult, Larsson, and Iversen (2000). Chlorite delignification was carried out using 1 mg of $NaClO_2$ for 1 g of dry pulp at pH 4 for 4 h at 70 °C. In acid hydrolysis samples were first treated with 2.5 M HCl at 100 °C for 17 h, after which they were washed with distilled water until the pH of the samples was 5. It has been reported earlier that cellulose fibril aggregate growth does not take place until at temperatures over 140 °C (Fahlen & Salmen, 2003), and therefore this pretreatment of the samples is not expected to have any influence on measured aggregate sizes. Effect of strong acid hydrolysis to cellulose ultrastructure has also been analysed by Hult (2001), it was noted that only notable change brought by this treatment was the partial conversion of cellulose I_α to I_β.

All spectra were recorded with Varian $^{\text{UNITY}}INOVA$ 300 spectrometer, each dataset was accumulated for 20 h. Acquisition time was 19 ms, contact time 1 ms, delay between pulses was 3 s, and sample rotation frequency 5 kHz. Resulting FID was multiplied with exponential function

$$g(t) = e^{-\alpha t} \quad (1)$$

with $\alpha = -10$ Hz in order to improve resolution of spectra. The measured spectra are presented in Fig. 2.

3.2. Carbohydrate analysis

Carbohydrate analysis of the pulps was performed according to Hausalo (1995) using 72 w% sulfuric acid pretreatment (strong hydrolysis) followed by hydrolysis at 4 w% as pretreatment and detection of the released monosaccharides by HPAEC/PAD. Total lignin content (Klason + acid soluble) was determined according to Browning (1967). Monosaccharide composition and lignin content of the samples are presented in Table 4. In order to determine if hemicelluloses were successfully removed from

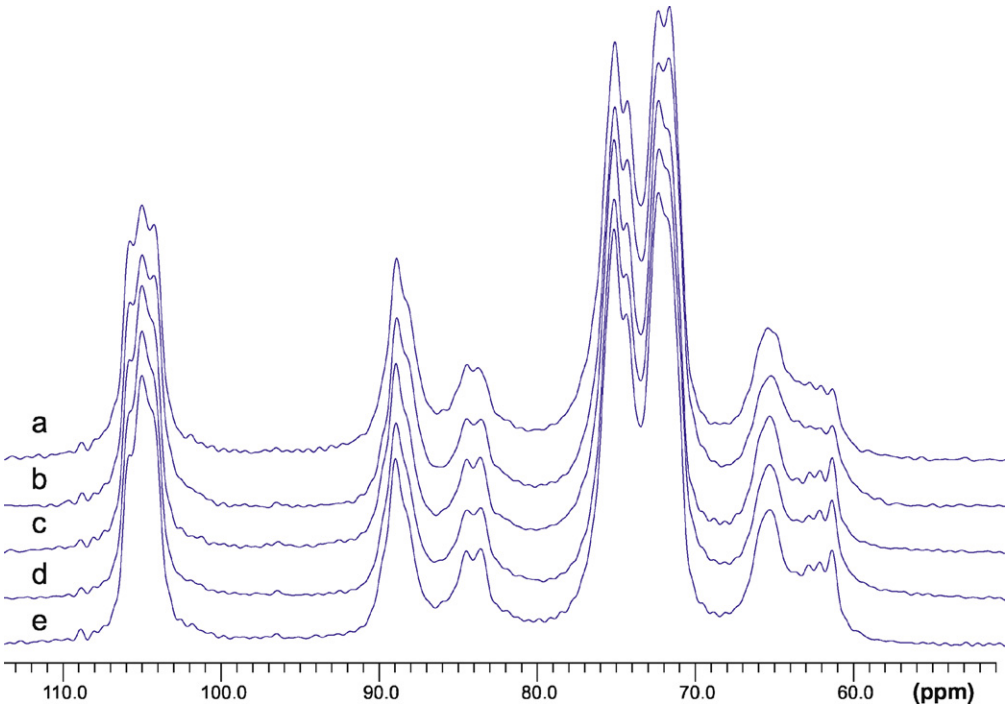

Fig. 2. ^{13}C CPMAS NMR spectra of kraft pulp samples from different cooking experiments: HiA at kappa level 50 and 30 (spectra a and b, respectively), LS (c) and Ref at kappa level 50 and 30 (d and e). Resolution enhancement of −10 Hz was used prior Fourier transform.

Table 4
Monosaccharide composition of pulp samples after cook

	Total lignin (%)	Monosaccharide composition (%)				
		Arabinose	Galactose	Glucose	Xylose	Mannose
LS	3.9	0.6	0.3	84.1	9.0	6.0
Ref	3.7	1.0	0.5	83.0	8.9	6.6
HiA130i180c	4.0	0.6	0.5	87.4	4.5	7.0
HiA90i180c	3.9	0.6	0.5	87.6	4.3	7.0
HiA90i160c	4.0	0.9	0.6	85.1	6.5	6.9
PS	3.7	1.0	0.6	81.6	9.3	7.5
PS-HiA	4.0	0.6	0.7	83.3	4.3	11.1

Table 5
Monosaccharide composition of pulp samples after strong acid hydrolysis prior NMR measurement

	Monosaccharide composition (%)					
	Arabinose	Galactose	Glucose	Xylose	Mannose	Rhamnose
LS	+[a]	+	97.6	0.9	1.5	–[b]
Ref	+	+	97.4	0.9	1.7	–
HiA130i180c	+	+	97.6	0.4	2.0	–

Detection limits for monosaccharides were 0.3 mg/100 mg (Ara, Gal, Glc, Xyl, Rham) and 0.5/100 mg (Man).
[a] +, below determination limit.
[b] –, not detected.

samples after acid hydrolysis prior NMR measurements, another carbohydrate analysis was performed to selected samples after the treatment. Monosaccharide composition for hydrolysed samples can be found in Table 5. It can be seen that glucose content for all included samples is >97%, which was regarded to be sufficient for spectral fitting to be carried out.

3.3. Spectral fitting

By comparing signal areas that originate from surface structures of cellulose fibril to the whole area of C(4) region it is possible to obtain an average value for number of cellulose chains in fibril surfaces. Assuming square cross section for fibrils and fibril aggregates, and using a conversion factor 0.57 nm for size of one cellulose chain (Newman, 1999a; Sugiyama, Vuong, & Chanzy, 1991) an average lateral dimension for cellulose fibrils and fibril aggregates can then be calculated. Method and model used for spectral fitting and fibril aggregates was that developed by Larsson et al. (with the exception of the lineshapes used in this work), and is described in detail elsewhere (Hult, 2001; Larsson, Wickholm, & Iversen, 1997; Wickholm, Larsson, & Iversen, 1998). In this model non-crystalline cellulose is considered to be located only on the surfaces of the fibrils, therefore the wide line at ~80 to 86 ppm consists solely of the signals contributed to accessible and inaccessible fibril surfaces. The deconvolution was performed by fitting seven lines to the C(4) region and using additional constraints for the areas of the lines that originate from cellulose I_α and I_β (VanderHart & Atalla, 1984; Yamamoto & Horii, 1993). Processing of spectral data and deconvolution process was performed using PERCH NMR Software (Laatikainen et al., 1996).

4. Results and discussion

In Fig. 3 a close-up of C(4)-region from the spectrum of reference pulp sample (Ref) and an example of performed deconvolution can be seen. In this figure individual deconvolution lines, experimental spectrum, and superimposed calculated spectrum from deconvolution can be seen. Results obtained from spectral fitting are presented in Table 6, and together with measured physical properties for Ref, PS, and HiA pulps in Table 7. From these results it can be seen that largest aggregate sizes are obtained with high alkalinity cook and lowest in reference cook. There is only a slight increase in fibril sizes with the change in kappa level from 50 to 30 while aggregate sizes remain unaffected. This is a consequence of the fact that major changes in

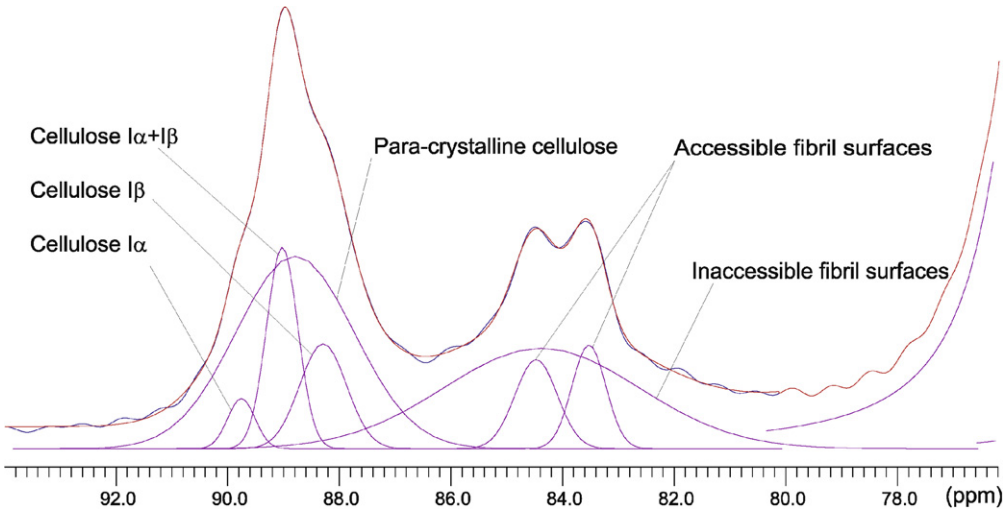

Fig. 3. Deconvolution of C(4) – signal from the spectrum of Ref. – cook sample. Only Gaussian lineshapes have been used in fitting process. Resolution enhancement of −10 Hz was used prior Fourier transform.

Table 6
Results obtained from spectral fitting

	Unbleached samples		Bleached samples	
	d_f	d_a	d_f	d_a
LS	4.77 (0.02)	19.2 (0.1)	4.66 (0.02)	21.34 (0.09)
Ref[a]	4.47 (0.01)/4.39 0.06)	18.2 (0.3)/18.5 (0.3)	4.55 (0.06)	19.9 (0.3)
HiA130i180c[a]	4.86 (0.03)/4.59 (0.11)	20.4 (0.2)/19.9 (0.6)	4.72 (0.12)	21.1 (0.6)
HiA90i180c	4.26 (0.08)	20.2 (0.5)		
HiA90i160c	4.37 (0.08)	20.9 (0.5)		
PS	4.19 (0.05)	19.5 (0.3)		
PS-HiA	4.23 (0.08)	18.7 (0.4)		

Lateral dimensions of fibrils and fibril aggregates are referred as d_f and d_a, respectively. All values are nanometers. Values given in parenthesis are standard errors for weighted averages.
[a] Data corresponding to kappa levels 30/50.

Table 7
Strength properties at tensile index 70 Nm/g

	Beating (revs.)	WRV (g/g)	Density (kg/m^3)	Tear index (mNm^2/g)	Zero span, wet (Nm/g)	Scott bond (J/m^2)	d_a (nm)[a]
Ref	1103	1.94	742	13.8	134	449	18.2
HiA130i180c	1787	1.83	700	16.1	141	296	20.4
HiA90i180c	1746	1.74	711	15.6	134	311	20.2
HiA90i160c	1737	1.82	738	15.9	136	459	20.9
PS	778	1.88	743	14.0	128	437	19.5
PS-HiA	801	1.84	714	14.1	133	327	18.7

[a] Aggregate sizes from spectral fitting, see Table 6.

aggregate sizes take place at the beginning of the cooking process (Hult et al., 2001). By comparing C(1) and C(4) regions (~100–110 ppm and ~80–90 ppm, respectively) in spectra from different pulp samples in Fig. 2 it can be seen that the high alkalinity pulps have the most prominent fine structure indicating higher level of ordering in fibers, which is in accordance with the results of lateral dimension calculations.

Since residual lignin was removed from all unbleached samples using chlorite treatment which was regarded to be a close equivalent to DEDED-bleaching, it was not expected to observe any differences in aggregate sizes between unbleached samples and those bleached with ODEDED-sequence. However, after ODEDED-bleaching a slight increase of aggregate size was observed. This suggests that the growth of the aggregates is related to the oxygen stage in ODEDED-sequence, possibly caused by the changes in the fiber structure due to the strong fluidicing mixing in alkaline conditions during that stage. In fibril sizes ODEDED-bleaching caused no systematic effect to be seen.

From the results for the high alkalinity temperature series it can be seen that changes introduced in impregnation temperature or in cooking temperature did not have any notable effect on aggregate size. Lowering of the cooking temperature was however accompanied by prolonged cooking time, which may explain similar aggregate sizes between these samples. When pulps that were cooked with added polysulfide were compared to corresponding reference and high alkalinity cooks, it was noted that there was a difference in aggregate growth between these cases. High alkalinity cook yielded an aggregate size of about two nanometers larger than what was obtained with reference cook, while in PS and PS-HiA pulps aggregate sizes were within error limits almost equal. It was thus concluded that increase in alkalinity does not lead to aggregate growth when polysulfide is present in the cook. From the sugar analysis presented in Table 4, it can be seen that in pulps obtained from polysulfide cooks there was a slightly higher amount of mannose present, which indicates a higher glucomannane content in these samples. It is possible that this higher hemicellulose content in polysulfide pulps leads to an inhibition of aggregate growth in applied cooking conditions.

Observed differences in average values for cellulose fibril aggregate sizes for pulp samples analysed in this study were at largest only about two nanometers, yet the pulps differed clearly in their physical properties. This suggests that aggregate size as such is not a crucial parameter to explain differences between pulp properties. It is to be noted that this is an opposite result than what was reported by Molin (2002), where tear index for pulps with different hemicellulose contents was correlated with aggregate sizes for those pulps. When similar correlation was performed with data obtained here (Fig. 4), it was noted that high alkalinity pulps (excluding PS-HiA) form their own group with a notably higher tear index values as compared to the rest of the pulps, and that the aggregate size has only a minor effect on tear index values in both groups (similar grouping can be observed when beating demand is correlated with

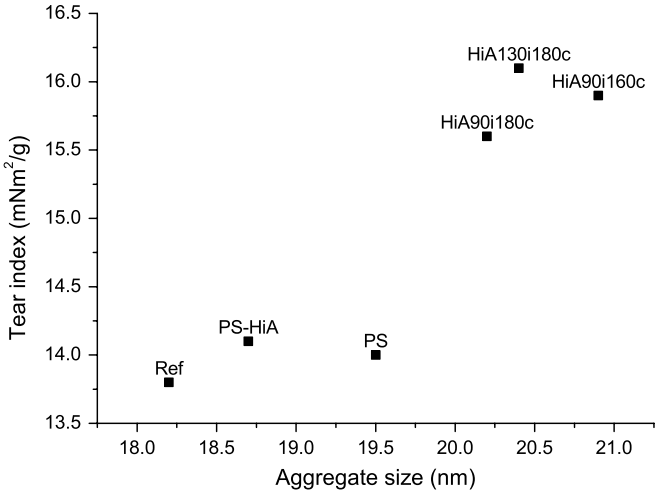

Fig. 4. Tear index at tensile 70 Nm/g of the pulp samples as a function of aggregate size.

aggregate size). This behaviour suggests that differences observed in tear index are mainly due to some other factor than fibril aggregate size. High alkalinity pulps, with the exception of PS-HiA, have a lower hemicelluloses content than the rest of the pulps, and it is likely that although in pulping conditions the loss of hemicelluloses facilitates fibril aggregation, the differences seen in tear index are related to the lowering of the hemicelluloses content by some other way. With other physical properties presented in Table 7 no such correlations with aggregate size were found.

The use of Lorentzian lines for modeling the signals originating from the highly crystalline domain in C(4) region together with Gaussian lines has been discussed in detail by Larsson and Westlund (2005). In this work however only Gaussian lineshapes were used. Attempts were made to include also Lorentzian lines according to given model, but with no success. Introducing variations to the the starting values (e.g. linewidth, intensity and line position) of the functions to be fitted did not resolve this problem, and it is possible that this discrepancy with the fitting model could be due to different algorithm used in fitting. Because of this values obtained here for aggregate and fibril sizes are probably not so accurate as those obtained with combined use of Gaussian and Lorentzian lines in the fitting process. Also the resolution enhancement (1) used in current work introduces distortions to the spectral lines, which affects calculated values for lateral dimensions. All studied spectra were however treated in the same manner, so obtained results are comparable within this work. The emphasis here is on finding differences between different pulp samples, and therefore the accuracy of the absolute values of aggregate sizes is only of little interest.

Care was taken to produce fits for each sample with as similar starting conditions as possible, however it turned out to be difficult to control all the effects that arise from, for example, applied baseline corrections and phase corrections to the spectra. Also the fitting process itself is rather subjective procedure and sensitive to variations in the starting values. Therefore for obtaining one fibril/aggregate size several fits were produced, and weighted average value for signal areas was then used in calculations. Errors in signal areas that arose from fitting process were combined together to yield the error in calculated lateral dimension using error propagation

$$\delta f \leq \sum_i \left|\frac{\partial f}{\partial x_i}\right| \delta x_i \qquad (2)$$

where δx_i are the individual errors and δf is the total error. It is worth noting however that when seven functions are used to describe the whole C(4) resonance, with each function having several free parameters to be fitted, the uniqueness of the solution obtained may very well be questioned (Atalla & VanderHart, 1999). Despite of the additional constraints used, reproducibility of the fits was still poor in some cases.

5. Conclusions

The application of solid state ^{13}C CPMAS NMR for structural analysis of kraft pulp fibers revealed a dependence of the cellulose fibril aggregate size on the variations in the kraft pulping conditions, with high alkalinity cook (HiA) giving the largest aggregate size. However, when this cooking experiment was analysed more thoroughly using different impregnation and cooking temperatures and addition of polysulfide in order to yield pulps with clear differences in their physical properties, no significant changes in cellulose aggregation was observed between these pulps. In polysulfide cooks changes in alkalinity level did not affect aggregate size. Since polysulfide is known to protect hemicelluloses from degradation in cooking process, this finding supports the assumption that enlargement of cellulose fibril aggregates during kraft pulping is at least partially dependent on effective removal of hemicelluloses. The fact that no clear correlations between cellulose fibril aggregate sizes and physical properties of the pulps was not observed suggests that the size of the fibril aggregates is not one of the key elements in determining the quality of pulp for paper making.

Acknowledgements

Finnish Funding Agency for Technology and Innovation (TEKES) is acknowledged for financing this study, which was carried out under the Bright Pulping project at KCL. The authors also thank Osmo Pekkala (KCL) for the description of the properties of the pulps from different cooking experiments.

References

Atalla, R., & VanderHart, D. (1999). The role of solid state^{13} C NMR spectroscopy in studies of the nature of native celluloses. *Solid State Nuclear Magnetic Resonance, 15*(1), 1–19.

Baird, M. S., O'Sullivan, A. C., & Banks, W. B. (1998). A native cellulose microfibril model. *Cellulose, 5*(2), 89–111.

Bardage, S., Donaldson, L., Tokoh, C., & Daniel, G. (2004). Ultrastructure of the cell wall of unbeaten Norway spruce pulp fibre surfaces. *Nordic Pulp and Paper Research Journal, 19*(4), 448–452.

Browning, B. L. (1967). *Methods of wood chemistry* (Vol. 2). New York: Interscience, pp. 785-791.

Duchesne, I., & Daniel, G. (2000). Changes in surface ultrastructure of Norway spruce fibres during kraft pulping – visualisation by field emission-SEM. *Nordic Pulp and Paper Research Journal, 15*(1), 54–61.

Duchesne, I., Hult, E.-L., Molin, U., Daniel, G., Iversen, T., & Lennholm, H. (2001). The influence of hemicellulose on fibril aggregation of kraft pulp fibres as revealed by FE-SEM and CP/MAS^{13} C NMR. *Cellulose, 8*(2), 103–111.

Duchesne, I., Takabe, K., & Daniel, G. (2003). Ultrastructural localisation of glucomannan in kraft pulp fibres. *Holzforschung, 57*(1), 62–68.

Evans, R., Newman, R. H., Roick, U. C., Suckling, I. D., & Wallis, A. F. (1995). Changes in cellulose crystallinity during kraft pulping. Comparison of infrared, X-ray diffraction and solid state NMR results. *Holzforschung, 49*(6), 498–504.

Fahlen, J., & Salmen, L. (2003). Cross-sectional structure of the secondary wall of wood fibers as affected by processing. *Journal of Materials Science, 38*(1), 119–126.

Fahlen, J., & Salmen, L. (2005). Ultrastructural changes in a holocellulose pulp revealed by enzymes, thermoporosimetry and atomic force microscopy. *Holzforschung, 59*(6), 588–597.

Hausalo, T. (1995). Analysis of wood and pulp carbohydrates by anion exchange chromatography with pulsed amperometric detection. In *8th International Symposium on Wood and Fibre and Pulping Chemistry proceedings*. Vol. 3, (pp. 131–136). Helsinki.

Hult, E. -L. (2001). *CP/MAS* ^{13} *C NMR spectroscopy applied to structure and interaction studies on wood and pulp fibers*. Ph.D. thesis, Royal Institute of Technology, Stockholm, Sweden.

Hult, E.-L., Iversen, T., & Sugiyama, J. (2003). Characterization of the supermolecular structure of cellulose in wood pulp fibres. *Cellulose, 10*(2), 103–110.

Hult, E.-L., Larsson, P., & Iversen, T. (2001). Cellulose fibril aggregation – An inherent property of kraft pulps. *Polymer, 42*(8), 3309–3314.

Hult, E.-L., Larsson, P. T., & Iversen, T. (2000). A comparative CP/MAS^{13} C NMR study of cellulose structure in spruce wood and kraft pulp. *Cellulose, 7*(1), 35–55.

Hult, E.-L., Liitiä, T., Maunu, S. L., Hortling, B., & Iversen, T. (2002). A CP/MAS^{13} C NMR study of cellulose structure on the surface of refined kraft pulp fibers. *Carbohydrate Polymers, 49*(2), 231–234.

Krässig, H. A. (1993). *Cellulose: Structure, accessibility and reactivity, volume 11 of polymer monographs*. Lausanne: Gordon and Breach.

Laatikainen, R., Niemitz, M., Weber, U., Sundelin, J., Hassinen, T., & Vepsäläinen, J. (1996). General strategies for total-lineshape type spectral analysis of NMR spectra using integral-transform iterator. *Journal of Magnetic Resonance, Series A, 120*(1), 1–10.

Larsson, P. T., & Westlund, P.-O. (2005). Line shapes in CP/MAS^{13} C NMR spectra of cellulose I. *Spectrochimica Acta Part A, 62*, 539–546.

Larsson, P. T., Wickholm, K., & Iversen, T. (1997). A CP/MAS^{13} C NMR investigation of molecular ordering in celluloses. *Carbohydrate Research, 302*(1-2), 19–25.

Lennholm, H., Larsson, T., & Iversen, T. (1994). Determination of cellulose I_α and I_β in lignocellulosic materials. *Carbohydrate Research, 261*(1), 119–131.

Liitiä, T., Maunu, S. L., & Hortling, B. (2000). Solid state NMR studies on cellulose crystallinity in fines and bulk fibres separated from refined kraft pulp. *Holzforschung, 54*(6), 618–624.

Molin, U. (2002). Pulp strength properties: Influence of carbohydrate composition, molar mass and crystalline structure. Ph.D. thesis, Royal Institute of Technology, Stockholm, Sweden.

Newman, R. H. (1999a). Estimation of the lateral dimensions of cellulose crystallites using^{13} C NMR signal strengths. *Solid State Nuclear Magnetic Resonance, 15*(1), 21–29.

Newman, R. H. (1999b). Estimation of the relative proportions of cellulose I_α and I_β wood by carbon-13 NMR spectroscopy. *Holzforschung, 53*(4), 335–340.

Newman, R. H., & Hemmingson, J. (1990). Determination of the degree of cellulose crystallinity in wood by carbon-13 nuclear magnetic resonance spectroscopy. *Holzforschung, 44*(5), 351–355.

Samejima, M., Sugiyama, J., Igarashi, K., & Eriksson, K.-E. L. (1998). Enzymatic hydrolysis of bacterial cellulose. *Carbohydrate Research, 305*(2), 281–288.

Sugiyama, J., Vuong, R., & Chanzy, H. (1991). Electron diffraction study on the two crystalline phases occurring in native cellulose from an algal cell wall. *Macromolecules, 24*(14), 4168–4175.

Teeäär, R., Serimaa, R., & Paakkari, T. (1987). Crystallinity of cellulose, as determined by CP/MAS NMR and XRD methods. *Polymer Bulletin, 17*(3), 231–237.

VanderHart, D. L., & Atalla, R. H. (1984). Studies of microstructure of native celluloses using solid-state^{13} C NMR. *Macromolecules, 17*(8), 1465–1472.

Wathen, R. (2006). *Studies on fiber strength and its effect on paper properties*. Ph.D. thesis, Helsinki University of Technology.

Wickholm, K., Larsson, P. T., & Iversen, T. (1998). Assignment of noncrystalline forms in cellulose I by CP/MAS^{13} C NMR spectroscopy. *Carbohydrate Research, 312*(3), 123–129.

Yamamoto, H., & Horii, F. (1993). CP/MAS^{13} C NMR analysis of the crystal transformation induced for valonia cellulose by annealing at high temperatures. *Macromolecules, 26*(6), 1313–1317.